

# DATA FOR SIMPLE ESTIMATES OF SHIELDING AGAINST NEUTRONS AT ELECTRON ACCELERATORS

K. TESCH

*Deutsches Elektronen-Synchrotron DESY, Hamburg, Germany*

*(Received July 3, 1978; in final form October 30, 1978)*

If an experimental setup at an electron accelerator or a storage ring is surrounded by a shield of only moderate thickness the neutron dose due to giant-resonance neutrons ( $E_n < 10$  MeV) may be higher than the dose due to high-energy neutrons ( $E_n > 10$  MeV). Therefore, data on medium-energy neutron production are compiled and spectra are given for neutrons produced with high-Z and low-Z targets. As the spectra are similar to those of radioactive neutron sources, dose-equivalent attenuation coefficients of the 5 most important shielding materials are measured with Cf- and Am-Be sources for application at electron accelerators. For the purpose of estimating the high-energy neutron dose in a similarly simple way, results of Alsmiller and Barish are supplied in a convenient parametrized version.

## 1 INTRODUCTION

For calculating the shielding of electron accelerators at higher energies, four radiation components should be considered. The electron-photon component of the electromagnetic cascade is generated by interaction of electrons with matter of sufficient thickness. Medium-energy neutrons with energies up to 10 MeV are produced in processes ( $\gamma, n$ ), ( $\gamma, 2n$ ), ( $\gamma, np$ ), mainly by photons with energies around 20 MeV (giant resonance). High-energy photons produce neutrons by interaction with quasi-deuterons in the nucleus or by pionic effects on nucleons. As these neutrons of  $E_n \gg 10$  MeV are more penetrating than giant-resonance neutrons of medium energy, it would be advisable to process both components separately. Last, not least, it is necessary to consider the myons in connection with the shielding design under small angles to the beam and at energies about 1 GeV.

It is relatively simple to compute the shielding against myons, as the production cross sections are well known and since interaction of myons with matter proves to be of a particularly simple nature. It is possible to specify formulas for the computation of their dose behind any desired shielding<sup>1</sup>.

The dose due to scattered radiation from the electromagnetic cascade is dominated by low-energy electrons and photons. Consequently it depends on target geometry to a larger extent than for the three other components. It would be advisable, therefore, to proceed from measured

results instead of from computations. Experiments have been carried out<sup>2</sup> where the dose has been measured in well-defined standard geometries and behind various absorbers, so that in most cases under actual practice the shielding against this component may be easily estimated.

Methods for the calculation of the shielding against high-energy photon-neutrons have been described by Alsmiller and collaborators. The calculation of the shielding for a 400-MeV accelerator<sup>3</sup> is particularly useful, as these results may also be applied for higher primary energies (and approximately also for somewhat lower primary energies). Therefore they are quoted under section 4 in a parametrized scheme. In many cases its use may substitute neutron-transport calculations of one's own, as anyway the major uncertainty in the field of shielding design does not lie in the computational method, but in the assumptions on the radiation source (mean beam loss per year at one point of the accelerator etc.).

Generally, accelerators are "totally" shielded, i.e., the dose equivalent rate outside the shield is very small. The dose rate outside thick shields is determined by the high-energy neutrons produced at the source because low- and medium-energy neutrons, although produced in greater numbers, are heavily attenuated. However, in practice, one is often called upon to design thin shields as, for example, in experimental areas or for an electron storage ring. Outside thin shields giant-resonance neutrons dominate the neutron dose equivalent

TABLE I

Thickness of shielding material behind which the dose equivalent due to medium-energy neutrons is equal to the one of high-energy neutrons.

material	thickness (cm)
iron	60
heavy concrete	45
ordinary concrete	75
sand	110

rate. Table I shows for a number of materials those thicknesses behind which the dose of high-energy neutrons is equal to the one of medium-energy neutrons; here the data of sections 4 respectively 2 and 3 have been used (angle of observation  $90^\circ$ ).

Consequently knowledge of the dose of medium-energy neutrons is also necessary to design a "thin" shielding. On that account we have compiled, under Section 2, those data which are known about their spectra and about their production rates. It is shown that the spectra in good approximation are similar to spectra of known radioactive neutron sources.

Little knowledge is available about the attenuation of the dose of medium-energy neutrons produced at electron accelerators. Therefore, we alternatively measured the dose attenuation parameters for neutron sources; the results for 5 materials are specified under Section 3.

## 2 SPECTRA OF MEDIUM-ENERGY NEUTRONS

Experimental or theoretical data on spectra and production rates of medium-energy neutrons are only sparsely available. Below a compilation is given of some results, which are useful for the purpose intended.

The spectrum of neutrons with energies above 0.01 MeV was calculated by Alsmiller *et al.*<sup>4</sup> for 150-MeV electrons and a "thick" tantalum target. This spectrum has been confirmed for energies above 1 MeV by measurements of Burgart *et al.*<sup>5</sup> Both results are shown in Figure 1. Experimental spectra of Kaushal *et al.* (85-MeV bremsstrahlung and lead target; Ref. 6) and Verbinsky and Burrus (33-MeV bremsstrahlung and lead target; Ref. 7) are also given; as these authors only state relative distributions, the curves are normalized to the results of Alsmiller/Burgart at 4 MeV. Bathow *et al.*<sup>8</sup> have measured spectra produced by 6.3-GeV bremsstrahlung in lead, copper, and heavy concrete.

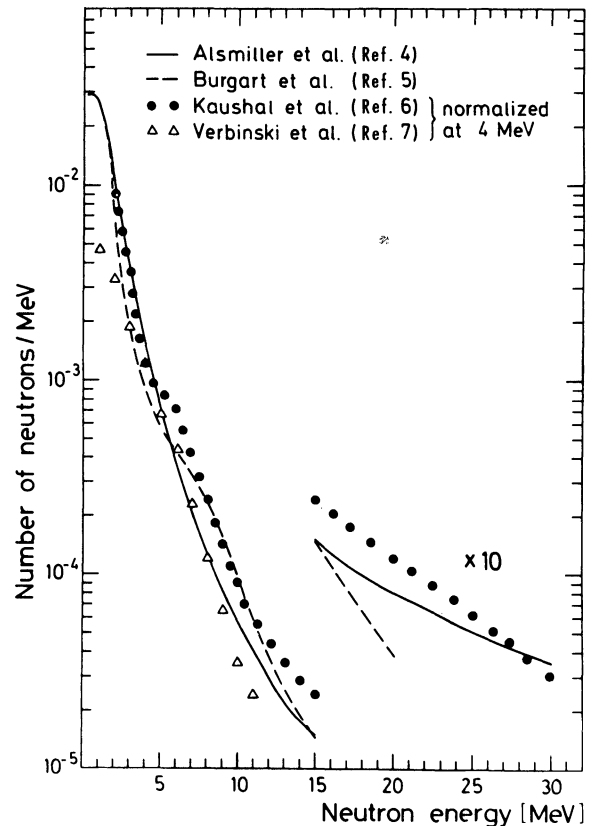


FIGURE 1 Spectra of medium-energy photoneutrons produced on a heavy target.

Neutrons produced on light nuclei have a broader spectrum. Figure 2 shows spectra from Refs. 6 and 7 for an aluminium target in arbitrary units, normalized to each other at 4 MeV.

In both illustrations the curves are in rather good agreement; the relative neutron distributions in the range of "evaporation neutrons," i.e., up to approximately 10 MeV, are essentially independent of primary energies. For targets of light and of heavy nuclei we can specify, therefore, suitable mean spectra, which are to be normalized on known production rates for neutrons up to 10 MeV.

Unfortunately, only few such production rates are known; they are compiled in Table II. The data give the number of neutrons with energies up to 10 MeV for an incident 1-GeV electron; it has been assumed here that these numbers are linearly dependent on the primary energy and that a target of optimal dimensions is used in which the cascade is fully developed, without absorption of neutrons. The data of line 1 have been determined with 6.3-GeV bremsstrahlung. The value in line 2 has

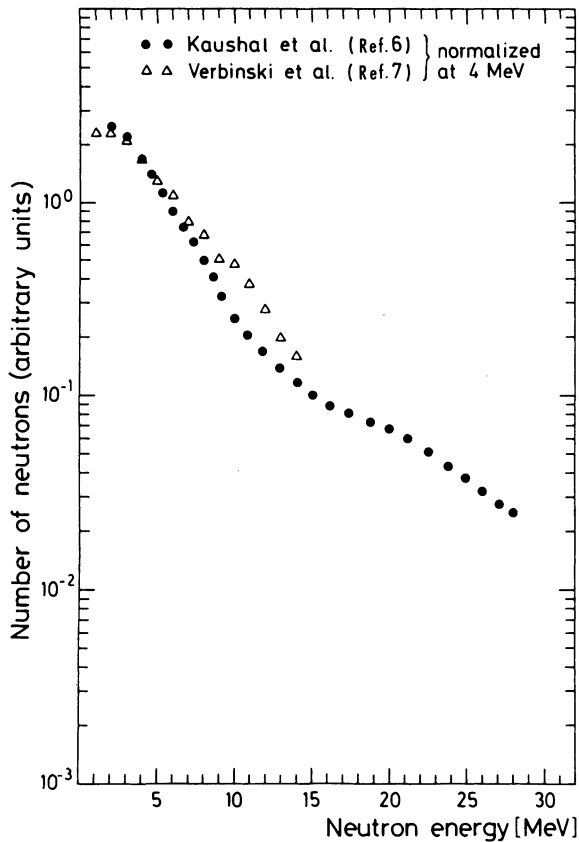


FIGURE 2 Spectra of medium-energy photon-neutrons produced on an aluminum target.

TABLE II

Number of neutrons with  $E_n < 10$  MeV, produced by one electron with energy 1 GeV.

target Refs.	$n/1\text{-GeV-e}$		
	Al	Cu	Ta, Pb
(8)	0.14	0.30	0.34
(4)			0.37
(9)			0.34
(10)	0.090	0.17	0.33
mean value	0.12		0.35

been obtained from the respective curve of Figure 1 by integration from 0 to 10 MeV.

The value of line 3 is a mean value derived from the work of Hansen *et al.*<sup>9</sup> in which production rates of 100-MeV electrons for tantalum and lead targets are compared using cross sections from some other papers.

Line 4 has been extracted from a paper of Swanson.<sup>10</sup> He computed production rates for

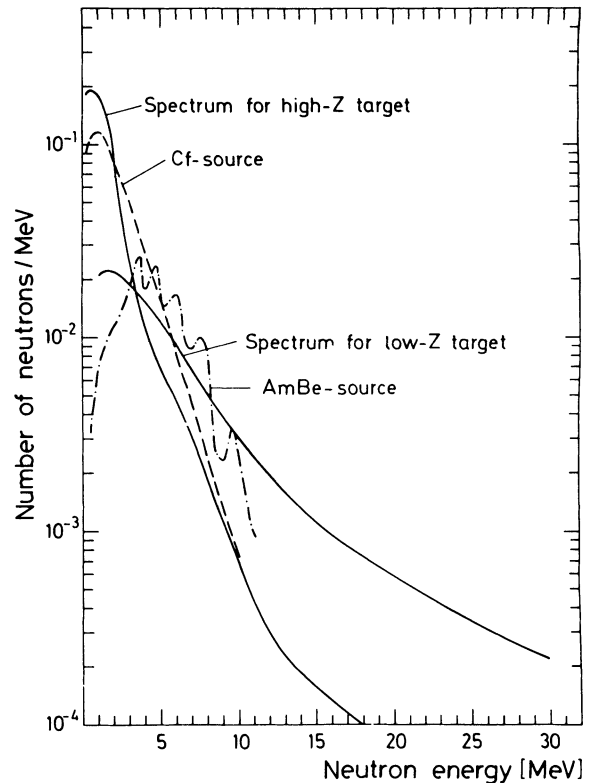


FIGURE 3 Spectral distributions of neutrons produced by one electron with an energy of 1 GeV. The spectra of radioactive neutron sources are shown for comparison.

lower electron energies (up to 100 MeV) and compared them with a number of experiments. (For other  $Z$ -values, he approximates the production rate by the expression  $9.3 \times 10^{10} Z^{0.73} n/s \text{ kW.}$ )

Now the mean spectra of neutrons photo-produced on light and on heavy targets are given in Figure 3 in such a way that the integration from 0 to 10 MeV will result in the mean values of Table II.

The curves can be approximated between 0.1 and approximately 10 MeV by the function

$$N(E)dE = A\sqrt{E} \exp(-E/T)dE. \quad (1)$$

This equation is practically equal to the expression of Lang and Le Couteur<sup>11</sup> from the evaporation model; a fission spectrum, too, may be described in good approximation by this expression (see further down below). For the parameters  $A$  and  $T$  the values in Table III are obtained in sufficient approximation. The mean energies of both spectra for neutron energies up to 10 MeV are also indicated; the effective energies referring to dose have practically the same values.

TABLE III  
Parameters for neutron spectra.

	A (MeV <sup>-1 2</sup> )	T (MeV)	$\bar{E}$ (MeV)
Al-target	0.030	3.0	3.9
heavy target	0.48	1.0	1.8
Am-Be-source			4.3
Cf-source			2.0

For comparison purposes Figure 3 additionally shows the spectra of known radioactive neutron sources. According to Knitter *et al.*<sup>12</sup> the fission spectrum of a <sup>252</sup>Cf source will be obtained by  $N(E) \sim \sqrt{E} \exp(-E/1.42)$ ,  $E$  measured in MeV. In the figure this spectrum has been normalized in such a way that the integral from 0 to 10 MeV yields the same value as for the photoneutrons from a heavy target. The two spectra are rather similar. This fact makes it possible to determine the data required to calculate the shielding against medium-energy neutrons simply by means of a neutron source. The spectrum of neutrons from an Al target is considerably broader; it resembles the spectrum of a <sup>241</sup>Am-Be source<sup>13,14</sup> (see Fig. 3). Therefore the dependence of shielding parameters on the spectrum can easily be studied with the two neutron sources mentioned.

### 3 SHIELDING PARAMETERS FOR MEDIUM-ENERGY NEUTRONS

If the spectrum of a neutron source is known, the dose of neutrons behind a shield may be computed, either by analytic methods or by Monte-Carlo calculations. Such calculations have been performed particularly for fission neutrons and their attenuation by ordinary concrete, see, e.g., Ref. 15. For practical protection purposes at accelerators, e.g., for the calculation of the shielding around experimental setups, these elaborate computations are often too cumbersome. Yet, they show that the dose attenuation is exponential in good approximation up to great depths; it will suffice, therefore, to know these dose attenuation coefficients for different materials actually used. It is useful if they do not include the distance dependence, i.e., apply to a constant source-measuring point distance. A build-up factor (approximately of magnitude 2) is only of minor interest, considering the inaccurate forecasts of accelerator operation.

As spectra of medium-energy giant-resonance neutrons are similar to those of radioactive neutron sources, we determined the dose attenuation coefficients of lead, iron, heavy concrete (magnetite concrete\*), ordinary concrete and sand for neutrons from a <sup>241</sup>Am-Be source and from a <sup>252</sup>Cf source.

The two sources had a source strength of  $3 \times 10^6$  respectively  $1 \times 10^7$  neutrons/s. The dose equivalent rate of neutrons was measured by a rem-meter after Anderson and Braun.<sup>16</sup> New measurements by Hankins<sup>17</sup> verify that this instrument records the dose equivalent within  $\pm 30\%$  in the energy range of 0.1 to 6 MeV. (In the range 1 keV to 100 keV the response is too high by a factor of 2 to 3.) The lateral dimensions of the absorbers could be varied between  $30 \times 30$  cm<sup>2</sup> and  $60 \times 60$  cm<sup>2</sup>. The distance source-instrument varied between 0.6 and 2.5 m. The entire setup was situated in the open at a height of 3.5 m to keep backscattering to a minimum.

Absorption curves have been measured for the materials mentioned above at various distances from the source, for various slab sizes and for both neutron spectra. We found that curves can be described by an exponential function and a build-up factor (magnitude 1.2 to 1.5), if for a constant source-dosemeter distance the arrangement of the absorbers is started from the source. If the absorbers are set up close to the instrument, a purely exponential decrease will be obtained in all cases. This effect is produced by the scattering effect of material near to the source. Also for reasons of "in-scattering" into the detector this attenuation coefficient depends on the slab size and the distance. Such effects are small for sand and concrete, but pronounced for iron and lead. Attenuation coefficients between 0.0026 and 0.0062 cm<sup>2</sup>/g can be obtained for lead.

The values of Table IV measured for larger distances and absorber dimensions  $60 \times 60$  cm<sup>2</sup>, are of practical interest; we assume that they also apply to larger lateral dimensions.

It has been ascertained by us that these coefficients are not influenced by back-scattering from the ground; this scattering only flattens out the exponential decrease as from a certain absorber thickness (40 to 60 cm in our setup). However, as computations show<sup>3,15</sup> that exponential attenuation continues up to very large thicknesses,

\* Composition as per parts by weight: Fe 0.50; O 0.34; Si 0.068; Ca 0.048; Mg 0.019; Al 0.010; H 0.004.

TABLE IV

Dose-equivalent attenuation coefficient  $\lambda$  for two neutron sources.

absorber	density (g/cm <sup>3</sup> )	$\lambda$ (cm <sup>2</sup> /g)	
		Cf source	Am-Be source
sand	1.6	0.033	0.027
ordinary concrete	2.3	0.027	0.021
heavy concrete	3.7	0.024	0.020
iron	7.8	0.0079	0.0079
lead	11.3	0.0044	0.0042

we are justified in using the coefficients also for thicker shields.

Values of ordinary concrete may be compared with those of other authors. Sauermann and Schäfer<sup>18</sup> come to 0.032 cm<sup>2</sup>/g with a Cf source and to 0.025 cm<sup>2</sup>/g with a Am-Be source. 0.029 cm<sup>2</sup>/g has been specified for monoenergetic neutrons of 3 MeV.<sup>19</sup>

Table IV shows that for sand and concrete the attenuation coefficients for the two neutron spectra are only very little different from each other; for iron and lead they are identical within the accuracy of the measurement. Therefore, according to the considerations of the previous section, it is possible to use the mean values of Table IV to compute the shielding against medium-energy neutrons at electron accelerators. For ordinary concrete this value is in agreement with Ref. 20 where values between 0.027 and 0.023 cm<sup>2</sup>/g are specified for electron accelerators of 55 and 85 MeV energy.

The values of iron and lead apply to absorbers of larger lateral dimensions. Frequently ducts through concrete walls of accelerators are closed by small lead or iron absorbers. Too high doses are obtained if their neutron attenuation is calculated by the aforementioned values. Our measurements show that for such small absorbers, surrounded by material of a higher attenuation coefficient, values of 0.010 cm<sup>2</sup>/g (iron) and 0.0062 cm<sup>2</sup>/g (lead) can be used.

Occasionally only little space is available to arrange for the shielding of experimental setups. Lead or iron is being used then for shielding purposes. If additional shielding against medium-energy neutrons is required, these materials may be combined with paraffin or wood. We examined various combinations of these substances, assembling alternately slabs of a heavy and of a light material of 5 cm thickness each. The dose attenuation is exponential in the mean here, too, and may be expressed by a mean attenuation

coefficient (cm<sup>-1</sup>). The following values have been obtained: paraffin ( $\rho = 1.0$  g/cm<sup>3</sup>) 0.109 cm<sup>-1</sup>; pine wood ( $\rho = 0.49$  g/cm<sup>3</sup>) 0.041 cm<sup>-1</sup>; lead/paraffin 0.100 cm<sup>-1</sup>; lead/wood 0.057 cm<sup>-1</sup>; iron/paraffin 0.112 cm<sup>-1</sup>.

A  $\gamma$ -dose due to photons produced by neutrons in the absorber will be obtained for absorbers of sand and of ordinary concrete behind the absorber in addition to the neutron dose. For smaller absorber thicknesses this contribution can be neglected. After Roussin and Schmidt<sup>14</sup> the ratio of  $\gamma$ -dose to neutron dose is approx. 0.01 at a thickness of 50 cm, 0.1 at 75 cm and 1 at 100 cm, for our neutron spectrum and for ordinary concrete.

With the data given in Sections 2 and 3 the dose behind a shield can be estimated in a simple way. For converting the fluence into dose in front of the shield we use the relation  $1 \text{ n/cm}^2 \sim 4.0 \times 10^{-8} \text{ rem}$ , according to a mean energy of 2 to 4 MeV.<sup>21</sup>

#### 4 SHIELDING ESTIMATES FOR HIGH-ENERGY NEUTRONS

As already stated, the dose of high-energy neutrons ( $E_n > 10$  MeV) may be estimated by a similarly simple method, using the work of Alsmiller and Barish.<sup>3</sup> These authors calculated the dose equivalent behind shieldings of sand, ordinary concrete, heavy concrete\* and iron for neutrons with energies above 15 MeV, produced by 400-MeV electrons on a copper target. It is assumed that in a point target the maximum number of neutrons will be generated, without being absorbed. For electron accelerators with energies above 100 MeV it will generally suffice to scale these data proportional to the beam power.

For practical purposes the results of Alsmiller and Barish may be given in the following expression:

$$D(\theta, r) = \frac{S(\theta)}{r^2} \cdot \exp(-\lambda(\theta)d). \quad (2)$$

Here the parameters  $S(\theta)$  and  $\lambda(\theta)$  are specified in Table V,  $D(\theta, r)$  being the neutron dose in rem produced by  $10^{10}$  electrons of the energy 1 GeV,  $r$  being the distance from the target in cm,  $d$  the

\* Ilmenite concrete with practically the same shielding properties as magnetite concrete specified under section 3.

TABLE V  
Parameters for Equation (2).

material	density (g/cm <sup>3</sup> )	S(rem cm <sup>2</sup> )				$\lambda$ (cm <sup>-1</sup> )			
		$\theta =$ 0-30	$\theta =$ 30-60	$\theta =$ 60-120	$\theta =$ 120-180	$\theta =$ 0-30	$\theta =$ 30-60	$\theta =$ 60-120	$\theta =$ 120-180
sand	1.6	0.75	0.68	0.50	0.28	0.017	0.018	0.018	0.020
ordinary concrete	2.3	0.75	0.68	0.50	0.28	0.023	0.025	0.025	0.028
heavy concrete	3.7	1.2	1.2	0.90	0.50	0.032	0.033	0.035	0.039
iron	7.8	2.0	1.8	1.3	0.78	0.032	0.032	0.032	0.032

thickness of the shielding in cm, and  $\theta$  being the angle against the direction of the electron beam.

$S$  is not a mere source term, but also incorporates a build-up factor and, moreover, makes allowance for the fact that the dose, decreasing exponentially in the shielding, is reduced at the end of the material due to lacking backscattering; consequently  $S$  is dependent on the material. The formula applies to shielding thicknesses being equal or larger than the values specified in Table I.

#### ACKNOWLEDGEMENT

I take this opportunity to thank H.-G. Ebeling and H. Janssen for the careful performance of the measurements mentioned in Section 3.

#### REFERENCES

1. W. R. Nelson, *Nucl. Instrum. Methods* **66**, 293 (1968); **120**, 401 and 413 (1974).
2. H. Dinter and K. Tesch, *Nucl. Instrum. Methods*, **143**, 349 (1977).  
A. Exposito *et al.*, *Nucl. Instrum. Methods*, **138**, 209 (1976).
3. R. G. Alsmiller and J. Barish, *Particle Accelerators*, **5**, 155 (1973).
4. R. G. Alsmiller *et al.*, *Nucl. Sci. Eng.*, **40**, 365 (1970).
5. C. E. Burgart, *et al.*, *Nucl. Sci. Eng.* **42**, 421 (1970).
6. N. N. Kaushal, *et al.*, *J. Nucl. Energy*, **25**, 91 (1971).
7. V. V. Verbinski and W. R. Burrus, *Phys. Rev.* **177**, 1671 (1969).
8. G. Bathow *et al.*, *Nucl. Phys.* **B2**, 669 (1967).
9. E. C. Hansen *et al.*, *J. Appl. Phys.* **46**, 1109 (1975).
10. W. P. Swanson, Stanford Linear Accelerator Center SLAC-PUB-2042 (1977).
11. K. J. LeCouteur, in *Nuclear Reactions*, edited by P. M. Endt and M. Demeur (North-Holland Publishing Company, Amsterdam, 1959), Vol. 1, Chap. VII.
12. H. H. Knitter, *et al.*, *Atomkernenergie* **22**, 84 (1973).
13. F. DeGuarrini and R. Malaroda, *Nucl. Instrum. Methods*, **92**, 277 (1971).
14. J. E. Lutkin and G. W. McBeth, *Nucl. Instrum. Methods*, **107**, 165 (1973).
15. R. W. Roussin and F. A. R. Schmidt, *Nucl. Sci. Eng.* **15**, 319 (1971).
16. I. O. Anderson and J. Braun, *Nukleonik* **6**, 237 (1964).
17. D. E. Hankins, *Congress Intern. Rad. Protection Assoc.* Paris, 1977.
18. P. F. Sauermaun and W. Schäfer, *Atompraxis* **14**, (1968).
19. J. J. Broerse and F. J. Van Werven, *Health Phys.*, **12**, 83 (1966).
20. National Council on Radiation Protection, Washington NCRP-49 (draft) 1975.
21. Recommendations of the International Commission on Radiological Protection, ICRP Publication 21, 1973.